

# Use of Culture Geometry to Control Hypoxia-Induced Vascular Endothelial Growth Factor Secretion from Adipose-Derived Stem Cells: Optimizing a Cell-Based Approach to Drive Vascular Growth

Matthew L. Skiles, PhD,<sup>1</sup> Suchit Sahai, PhD,<sup>1</sup> Lindsay Rucker,<sup>1</sup> and James O. Blanchette, PhD<sup>1,2</sup>

Adipose-derived stem cells (ADSCs) possess potent angiogenic properties and represent a source for cell-based approaches to delivery of bioactive factors to drive vascularization of tissues. Hypoxic signaling appears to be largely responsible for triggering release of these angiogenic cytokines, including vascular endothelial growth factor (VEGF). Three-dimensional (3D) culture may promote activation of hypoxia-induced pathways, and has furthermore been shown to enhance cell survival by promoting cell-cell interactions while increasing angiogenic potential. However, the development of hypoxia within ADSC spheroids is difficult to characterize. In the present study, we investigated the impact of spheroid size on hypoxia-inducible transcription factor (HIF)-1 activity in spheroid cultures under atmospheric and physiological oxygen conditions using a fluorescent marker. Hypoxia could be induced and modulated by controlling the size of the spheroid; HIF-1 activity increased with spheroid size and with decreasing external oxygen concentration. Furthermore, VEGF secretion was impacted by the hypoxic status of the culture, increasing with elevated HIF-1 activity, up to the point at which viability was compromised. Together, these results suggest the ability to use 3D culture geometry as a means to control output of angiogenic factors from ADSCs, and imply that at a particular environmental oxygen concentration an optimal culture size for cytokine production exists. Consideration of culture geometry and microenvironmental conditions at the implantation site will be important for successful realization of ADSCs as a pro-angiogenic therapy.

## Introduction

**T**HERAPIES THAT STIMULATE regeneration of damaged tissues in the body or restore deficient tissues with bioengineered replacements represent an appealing and emerging technology. Such therapies often involve the implantation of cells or tissue into an ischemic wound environment, necessitating rapid vascularization for survival and integration of the implant. Indeed, diffusional mass transfer limitations restrict the potential size of engineered tissues and remain one of the biggest challenges to their clinical success.<sup>1,2</sup> New strategies to enhance angiogenesis are required to overcome these hurdles.

Strategies that harness the angiogenic potential of cells have shown promising results in recent studies. Fibroblasts<sup>3,4</sup> and mesenchymal stem cells<sup>5-7</sup> can significantly contribute to endothelial network formation and maintenance of micro-

vasculature. Dispersed mesenchymal stromal cells implanted in dermal wounds<sup>8,9</sup> and ischemic tissue<sup>10,11</sup> increased local levels of angiogenic cytokines and promoted increased capillary density. Of the potential cell candidates to be utilized for cell-based delivery, adipose-derived stem cells (ADSCs) appear particularly well suited for use in regenerative medicine due to their relative abundance and ease of culture as well as their ability to differentiate into relevant cell types in musculoskeletal tissue engineering (e.g., osteoblasts, chondrocytes, vascular smooth muscle cells).

The manner of cell transplantation to an injury site can impact transplant performance. Cells injected as dispersion have reduced cell-cell and cell-matrix interactions which are important in sustaining prosurvival pathways and suppressing apoptosis.<sup>11,12</sup> Alternatively, three-dimensional (3D) cultures retain these interactions, while also providing reduced oxygen tension within the cell mass, which may prime

<sup>1</sup>Biomedical Engineering Program, and <sup>2</sup>Department of Chemical Engineering, College of Engineering and Computing, University of South Carolina, Columbia, South Carolina.

the cells for the ischemic implantation site,<sup>13–15</sup> enhancing therapeutic effect. For example, cord blood mesenchymal stem cells implanted as 3D spheroids upregulated expression of anti-apoptotic and angiogenic proteins, downregulated expression of pro-apoptotic proteins, and showed superior integration into newly forming vessels in ischemic mouse hind limbs compared to dispersed cells.<sup>15</sup>

Oxygen gradients that form within 3D tissues are not necessarily detrimental. For instance, hypoxia is responsible for initiating angiogenesis *in vivo*<sup>16,17</sup> through activation of hypoxia-inducible transcription factors (HIFs) and subsequent upregulation of bioactive factors, such as vascular endothelial growth factor (VEGF).<sup>18–21</sup> HIF proteins are dimeric transcription factors of the basic helix-loop-helix-Per-Arnt-Sim family each composed of an  $\alpha$  and  $\beta$  subunit.<sup>22</sup> The  $\alpha$  subunit undergoes oxygen-dependent hydroxylation, marking it for proteosomal degradation. When local oxygen concentrations are not adequate for hydroxylation to occur, the subunit is stabilized, pairs with a  $\beta$  subunit, and is free to bind to hypoxia-responsive elements (HREs) found in the promoter region of a number of genes involved in adapting the cell for survival in low oxygen.

Thus, oxygen tension in 3D cell masses can contribute to activation of HIF-regulated pathways which benefit the cells. For instance, HIF stabilization and VEGF upregulation in growing avascular tumors is well known to promote tumor vascularization.<sup>23,24</sup> Similarly, endothelial cells cultured as spheroids were found to express higher levels of HIF-1 $\alpha$  RNA than those cultured as a monolayer under the same oxygen conditions.<sup>25</sup> Additionally, hypoxia is known to play a role in regulating cell differentiation. During formation of vascularized endochondral bone, regional hypoxia leads to HIF activation and VEGF upregulation and is integral for the formation of a cartilage template and synchronization of ossification with angiogenesis.<sup>26,27</sup> Thus, it is clear that identifying approaches to regulate desirable, HIF-activated signaling in ADSCs could provide new avenues towards creation of vascularized tissue and repair of critical size defects in bone.

The present study investigates the ability to control VEGF secretion from ADSCs by regulating hypoxic status. The effects of culture dimensions and incubator oxygen tension (atmospheric conditions as well as a pair of hypoxic levels) on angiogenic potential of ADSC spheroids are examined. HIF activity within the spheroids, identified using a previously-described fluorescent marker system,<sup>28</sup> was compared to levels of VEGF secretion from the cells. The impact of pelleting and hypoxia on cell viability and morphology were examined by staining and histological analysis. Results from this study provide insight into the nature of hypoxia in 3D cultures and may suggest a relevant approach for tailoring the release of angiogenic factors from ADSCs for improved vascularization of engineered tissues.

## Materials and Methods

### Cell culture

Passage 1 human ADSCs isolated from lipoaspirates were purchased from Invitrogen (Carlsbad, CA) and cultured in Complete MesenPRO RS<sup>TM</sup> reduced-serum medium supplemented with a penicillin-streptomycin solution (Mediatech, Manassas, VA; final concentration: 115 IU/mL penicillin,

115  $\mu$ g/mL streptomycin). This medium was also used throughout all experiments. For passaging, cells were kept in a humidified atmosphere of 95% air and 5% carbon dioxide at 37°C. Medium was changed thrice a week. At ~80% confluence, the cells were trypsinized and sub-cultured at a ratio of 1:4 until reaching passage 6, as recommended by the supplier. All data included in these studies were obtained from cells between passages 3 and 6. Maintenance of ADSC stemness was verified by cell-surface staining and flow cytometry. Purchased, P1 cells were >95% positive for stem cell surface markers CD44 and CD105. Fluorescent antibody labeling for each (CD44; eBioscience, San Diego, CA; CD105; Biolegend, San Diego, CA) revealed >95% staining for both markers at P6 (Supplementary Fig. S1; Supplementary Data are available online at [www.liebertpub.com/tea](http://www.liebertpub.com/tea)).

Nitrogen-purged, programmable incubators (Napco Series 8000, Thermo Electron, Waltham, MA) were used to maintain low oxygen levels for hypoxic culture studies. For 2% and 1% oxygen studies, all media, buffers, and fixatives to be used with the cells were kept in vented tubes in the corresponding incubator overnight before use to equilibrate the solutions to the appropriate oxygen concentration.

### Hypoxia marker virus

We have previously described the recombinant adenovirus used in this study to identify HIF activity.<sup>28</sup> Briefly, the virus was generated using the pAdEasy-1 system (QBiogene, Montreal, Canada) by inserting into the vector a destabilized variant of the red fluorescent protein, DsRed, (termed DsRed-DR) under the control of a minimal SV40 promoter and an HRE trimer. Previous ADSC studies have indicated ~100% infection efficacy using a multiplicity of infection of 80 (data not shown), which was utilized in these studies.

### ADSC infection and 3D culture formation

At ~80% confluence, ADSCs were trypsinized, centrifuged, resuspended in growth medium and counted. For HIF activity tracking studies, hypoxia marker virus was added to suspended cells and gently mixed for 30 min. ADSC spheroids of four different sizes were prepared by centrifugal pelleting. Five thousand (5k), 10,000 (10k), 20,000 (20k), or 60,000 (60k) cells were pipetted into 0.5 mL, screw-cap microcentrifuge tubes and centrifuged at 500 rcf for 2 min. Spontaneous aggregation of the pelleted cells into cohesive spheroids occurred during overnight incubation at 37°C. Spheroids of each size were then divided into three groups for incubation in 20%, 2%, or 1% O<sub>2</sub>. While in incubation, the tube caps were loosened slightly to allow for gas transfer. Medium was changed daily.

Spheroids for HIF activity tracking studies were encapsulated in polyethylene glycol by methods identical to those that have been published previously.<sup>28</sup> For reference, a video demonstration of this method by the authors is suggested.<sup>29</sup>

### Quantification of secreted VEGF

For secretion studies, spheroids were cultured in a volume of media based on cell number. 60k, 20k, 10k, and 5k spheroids were cultured in 900, 300, 150, and 75  $\mu$ L of medium, respectively. 60,000 cells grown in monolayer were also cultured at each oxygen concentration in 1 mL of

medium. Every 24h, the medium was removed from each sample and replaced with fresh medium. Media samples were stored at  $-80^{\circ}\text{C}$  before analysis. Levels of VEGF in media samples were determined by ELISA (Abcam, Cambridge, MA) following the manufacturer's instructions. For each group, six independent samples were analyzed.

#### Analysis of cell viability and morphology

Cell viability in ADSC spheroids was examined using a LIVE/DEAD cytotoxicity/viability assay (Invitrogen) and by histological examination. The LIVE/DEAD kit was used according to the manufacturer's instructions to identify esterase activity in live cells and loss of plasma membrane integrity in dead cells. For histological analysis of morphology, spheroids were first fixed overnight in a 4% paraformaldehyde solution. The spheroids were then embedded in 2% agar, paraffin processed, and cut into  $5\ \mu\text{m}$  sections. Sections were stained with hematoxylin and eosin and imaged.

#### Fluorescent cell imaging and image analysis

Imaging for spheroid size determination and fluorescent detection of the hypoxia marker was performed on a Nikon Eclipse Ti inverted fluorescent microscope (Nikon Instruments, Melville, NY) and image processing and analysis were performed in NIS-Elements software (Nikon Instruments). Identical camera and microscope settings were used for each capture within a study. Spheroids were imaged immediately after encapsulation, and then every 24h thereafter. Histological sections were imaged on a Nikon Optiphot-2 microscope (Nikon) fitted with a Zeiss AxioCam MRC camera (Carl Zeiss, Oberkochen, Germany).

For determination of spheroid sizes, the cross-sectional area of spheroids was measured in the software from representative, central-plane images of spheroids from each size group and the diameter of a circle with an equivalent area was calculated. Results are reported as the mean  $\pm$  standard deviation of six independent samples. To roughly quantify hypoxia marker signal, a fluorescent signal threshold intensity was applied to representative images from each group. The area of signal meeting or exceeding the threshold value was compared to the total spheroid area as calculated from the image. The threshold value was chosen such that no signal was detected in monolayer cells incubated in 20%  $\text{O}_2$ ,

as levels of HIF-1 $\alpha$  in these cultures were below detectable limits by western blotting in previous studies.<sup>30</sup>

#### Statistical analysis

All values are reported as mean  $\pm$  standard deviation of replicate samples. Statistical significance of differences between samples was determined by a two-tailed student's *t*-test assuming unequal variances ("\*\*\*" indicates statistical significance at  $p \leq 0.01$ , "\*\*" indicates statistical significance at  $p \leq 0.05$ ).

## Results

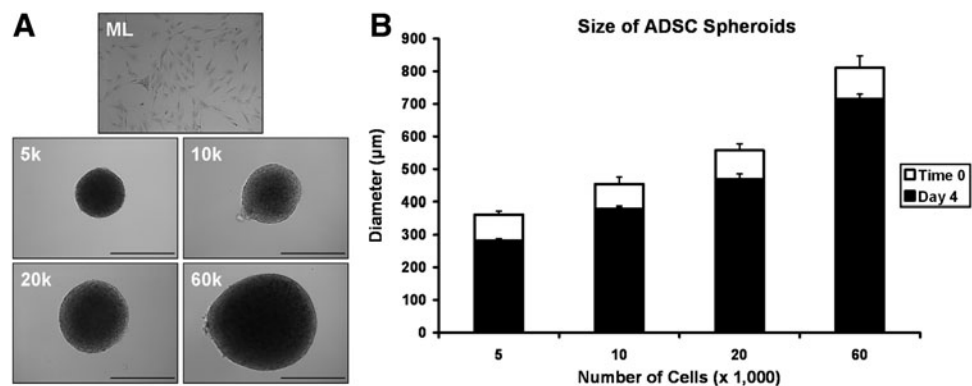
### Pelleted ADSCs form spherical, 3D cultures of reproducible size

After centrifugation, ADSCs formed a small plaque at the tip of each microcentrifuge tube. After overnight incubation, the cells had spontaneously condensed into round spheroids with a diameter dependent upon the initial number of cells. Figure 1A shows representative spheroids of each size at Time 0. ADSC spheroids were cohesive and consistently sized within each group. In Figure 1B the average diameter for spheroids from each study group at Time 0 (white bar) and at Day 4 (black bar) is shown. Minimum spheroid diameter was achieved by Day 4 with no further condensation observed thereafter. 5k, 10k, 20k and 60k spheroids were  $362 \pm 10\ \mu\text{m}$ ,  $454 \pm 21\ \mu\text{m}$ ,  $557 \pm 20\ \mu\text{m}$ , and  $811 \pm 37\ \mu\text{m}$  in diameter, respectively, immediately after formation. Spheroid diameters on Day 4 were  $282 \pm 6\ \mu\text{m}$ ,  $379 \pm 8\ \mu\text{m}$ ,  $469 \pm 16\ \mu\text{m}$ , and  $714 \pm 15\ \mu\text{m}$ , respectively. The ratio of spheroid size on Day 4 to initial spheroid size was similar for all size groups, ranging from  $\sim 78\%$  for 5k spheroids to  $88\%$  for 60k spheroids. Differences in culture oxygen concentration did not appear to have an effect on spheroid condensation.

### Spheroid size and external $\text{O}_2$ concentration affect regional hypoxic signaling

The degree of HIF activity in ADSC spheroids as indicated by fluorescent signaling of the HIF marker is shown in Figure 2. In spheroids of all sizes, HIF activity increased as incubator oxygen concentration decreased. With decreasing oxygen, signal onset was more rapid and signal area and intensity were increased. Signal also increased with spheroid

**FIG. 1.** (A) Representative adipose-derived stem cell (ADSC) monolayer and spheroid images for cultures formation from differing numbers of cells. (B) Diameter of spheroids formed by centrifugally pelleting different numbers of ADSCs. Initial spheroid size could be reliably controlled by adjusting the number of cells pelleted (white bars). Spheroids continued to condense for several days after initial formation before reaching a final minimal diameter by Day 4 (black bars). Scale bar =  $500\ \mu\text{m}$ .



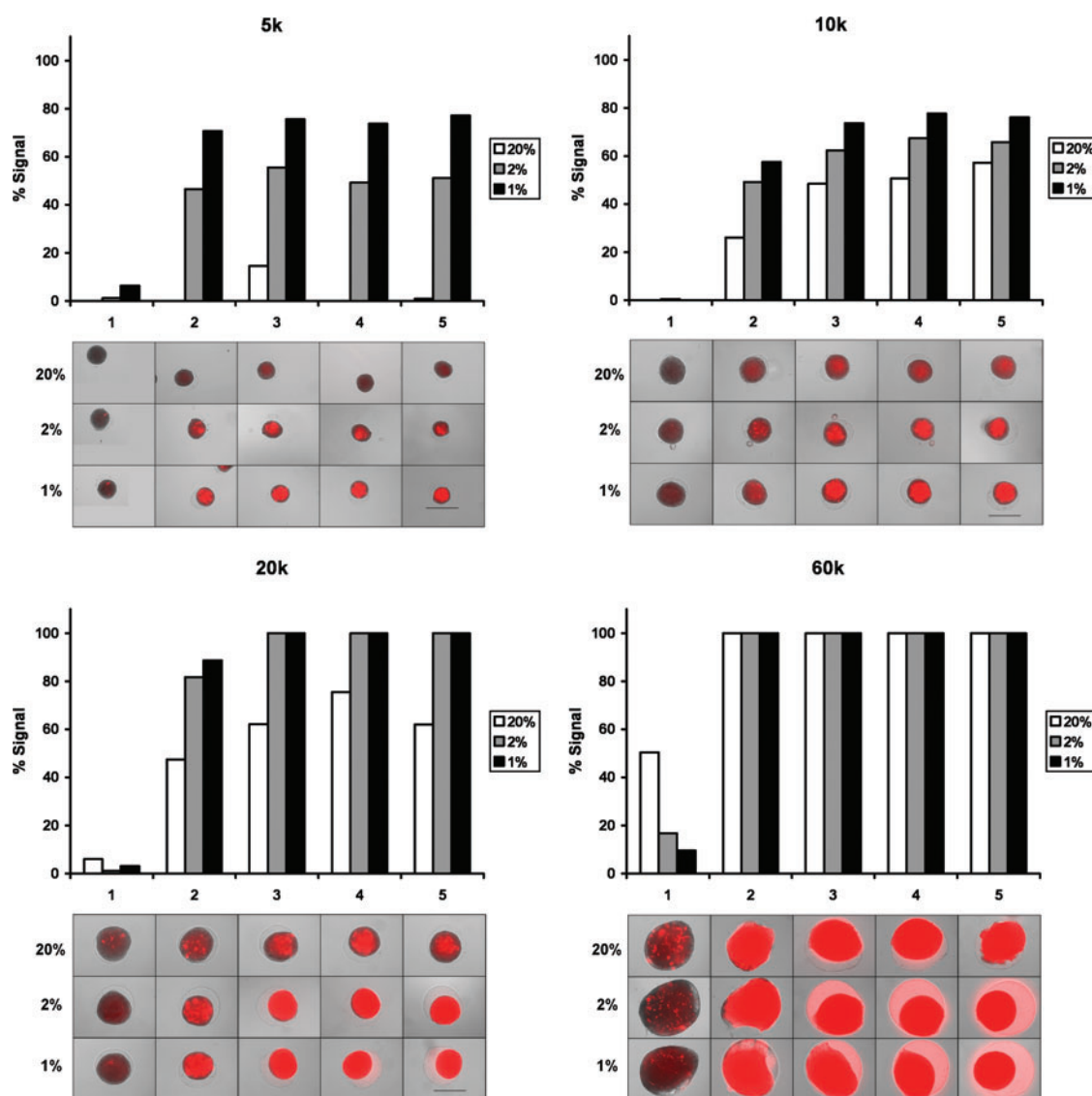


**FIG. 2.** Fluorescent DsRed signaling as an indicator of hypoxia-inducible transcription factor activity over 5 days in 5k (top left), 10k (top right), 20k (bottom left), and 60k (bottom right) ADSC spheroids incubated in 20%, 2%, or 1% O<sub>2</sub>. The relative extent of signaling is quantified in the graph above each set of figures by applying a signal intensity threshold value. The voided region caused by spheroid condensation can be seen as a ring in the hydrogel around the culture in some images. Scale bar = 500  $\mu$ m. Color images available online at [www.liebertpub.com/tea](http://www.liebertpub.com/tea)

size. 5k spheroids incubated in 20% O<sub>2</sub> displayed little or no signal over 5 days. Increasingly more signal was seen in 20% O<sub>2</sub> spheroids as spheroid diameter increased. For each oxygen concentration, signal onset was more rapid and signal area and intensity were higher as spheroid diameter increased. In general, signal was first observed in central regions of the spheroids and remained most intense there.

To roughly quantify the prevalence of HIF activity throughout the spheroids, an intensity threshold was applied to each image to identify regions exceeding it. The areas of these regions were compared to the total spheroid cross-sectional areas as determined in the software (graphs in Fig. 2).

The capture settings used in Figure 2 resulted in some spheroids with high levels of HIF activity being overexposed. In this case, differences in signal intensity between overexposed spheroids could be resolved by reducing the

camera exposure time (Supplementary Fig. S2). Though useful in identifying differences in HIF activity in spheroids that exceeded the dynamic range of capture at the given settings, apparent signal intensities measured from those images cannot be compared to intensities in Figure 2.

#### *Degree of hypoxia impacts VEGF secretion profile*

Figure 3 displays per-cell VEGF secretion from ADSCs in monolayers and spheroids cultured under different oxygen concentrations. The calculated mean values and standard deviations are reported in Table 1. Released VEGF values represent total release over the 24h before the stated time point. For each culture size, cells secreted significantly more VEGF when cultured in 2% or 1% O<sub>2</sub> than in 20% O<sub>2</sub>, while little significant difference was observed between 2% and 1% O<sub>2</sub>. In 2% and 1% O<sub>2</sub> culture, monolayers and 5k spheroids

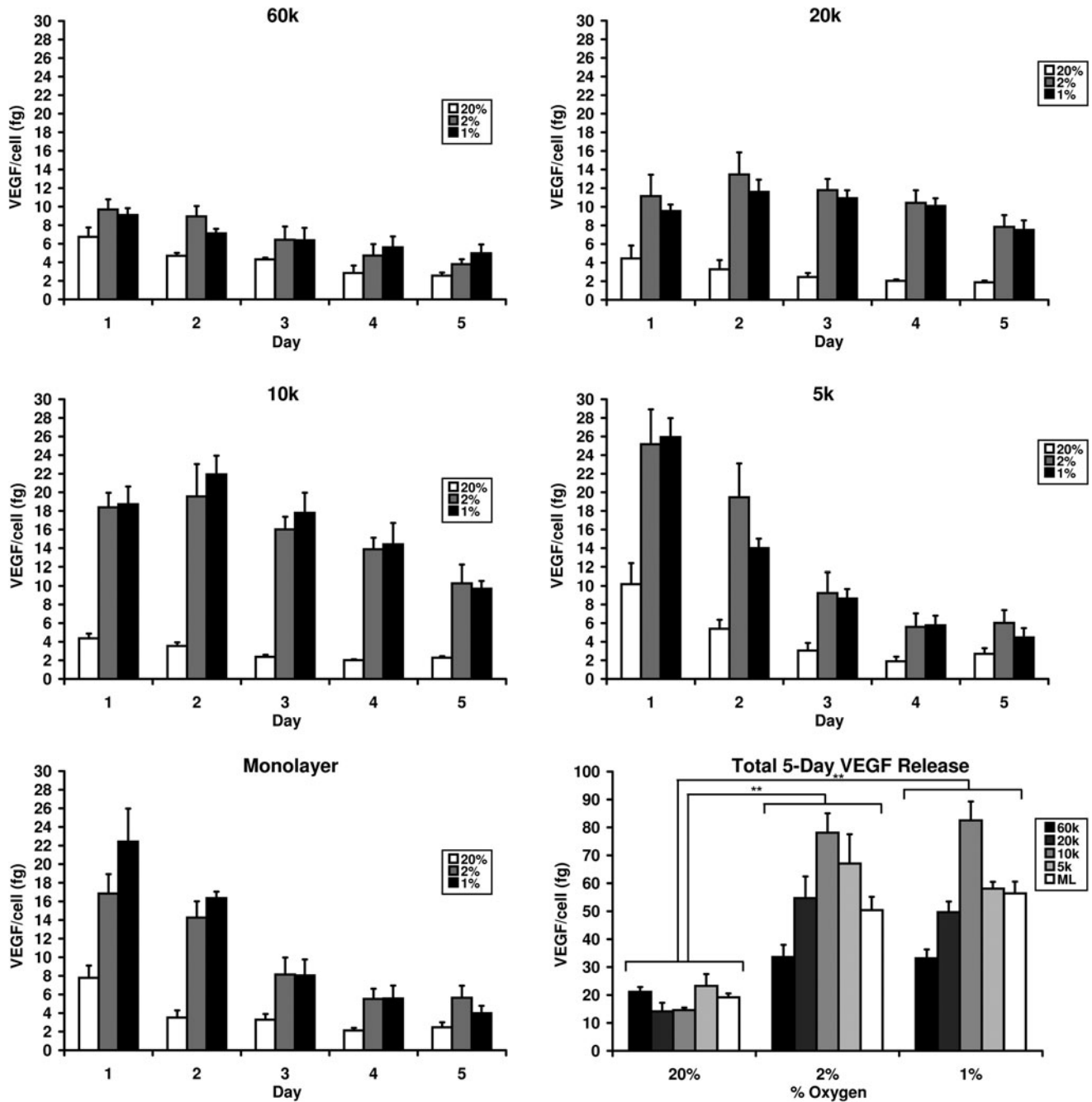


FIG. 3. Levels of daily and total per-cell vascular endothelial growth factor (VEGF) release from ADSC monolayers and 5k, 10k, 20k, and 60k spheroids incubated for 5 days in 20%, 2%, or 1% O<sub>2</sub>. (\*\* indicates statistical significance at  $p \leq 0.01$ ).

displayed significantly elevated VEGF secretion on Day 1 followed by a sharp decline through Day 5. Under the same conditions, 10k and 20k spheroids displayed a much more sustained elevation in VEGF secretion over 5 days, with peak secretion occurring on Day 2. 60k spheroids showed minor elevation of VEGF secretion on Day 1 which decreased over the remaining days. Total 5-day secretion was similar in 2% and 1% O<sub>2</sub> culture, which were both significantly higher than 20% O<sub>2</sub> culture. Total per-cell VEGF release increased from monolayers to 5k spheroids and from 5k to 10k spheroids then decreased from 10k to 20k spheroids and from 20k to 60k spheroids. Statistical significance of differences in VEGF

release between the different study groups can be found in Supplementary Table S1.

*Impact of hypoxia on morphology and viability*

The morphology of stained spheroid sections is shown in Figure 4a–h. On Day 1, all spheroids appeared cellular and cohesive throughout (a–c). After 5 days of culture in 20% O<sub>2</sub>, little morphological change was observed in most spheroids, though 60k spheroids did display a small central region of cells exhibiting cytoplasmic swelling (h). In 2% O<sub>2</sub>, the region with cytoplasmic swelling in 60k spheroids was much larger

TABLE 1. MEAN VALUES AND STANDARD DEVIATION OF VEGF RELEASE FROM ADSC CULTURES

%O <sub>2</sub>	Size	VEGF (fg)						Total
		Day						
		1	2	3	4	5		
20%	ML	7.8±1.3	3.5±0.8	3.3±0.6	1.9±0.3	2.3±0.5	18.8±1.4	
2%		16.8±2.1	14.2±1.7	8.1±1.8	5.1±1.0	5.2±1.2	49.5±4.6	
1%		22.1±3.5	16.4±0.7	8.0±1.7	5.1±1.3	3.2±0.6	54.8±4.1	
20%	5k	10.2±2.2	5.4±1.0	3.1±0.8	1.9±0.5	2.7±0.6	23.2±4.3	
2%		25.2±3.7	19.5±3.6	9.2±2.2	5.6±1.4	6.0±1.4	63.9±7.7	
1%		25.9±2.0	14.0±1.0	8.6±1.0	5.8±1.0	4.5±1.0	58.9±1.6	
20%	10k	4.4±0.5	3.5±0.4	2.4±0.2	2.0±0.1	2.3±0.2	14.6±0.9	
2%		18.4±1.6	19.6±3.5	16.0±1.4	13.9±1.2	10.3±2.0	78.1±6.9	
1%		18.7±1.9	21.9±2.0	17.8±2.2	14.4±2.3	9.7±0.8	82.5±6.8	
20%	20k	4.5±1.4	3.3±1.0	2.5±0.4	2.0±0.1	1.9±0.2	14.1±3.1	
2%		11.1±2.3	13.5±2.4	11.8±1.2	10.4±1.4	7.8±1.3	54.7±7.8	
1%		6.5±0.7	11.6±1.3	10.9±0.8	10.1±0.8	7.5±1.0	49.7±3.8	
20%	60k	6.7±1.0	4.7±0.3	4.3±0.2	2.8±0.8	2.5±0.3	20.6±1.2	
2%		9.7±1.1	8.9±1.1	6.4±1.4	4.7±1.2	3.8±0.5	34.0±4.8	
1%		9.1±0.7	7.1±0.5	6.4±1.3	5.6±1.2	5.0±0.9	33.9±2.9	

Statistical significance of differences between groups is indicated in Supplementary Table 1. ADSCs, adipose-derived stem cells; VEGF, vascular endothelial growth factor.

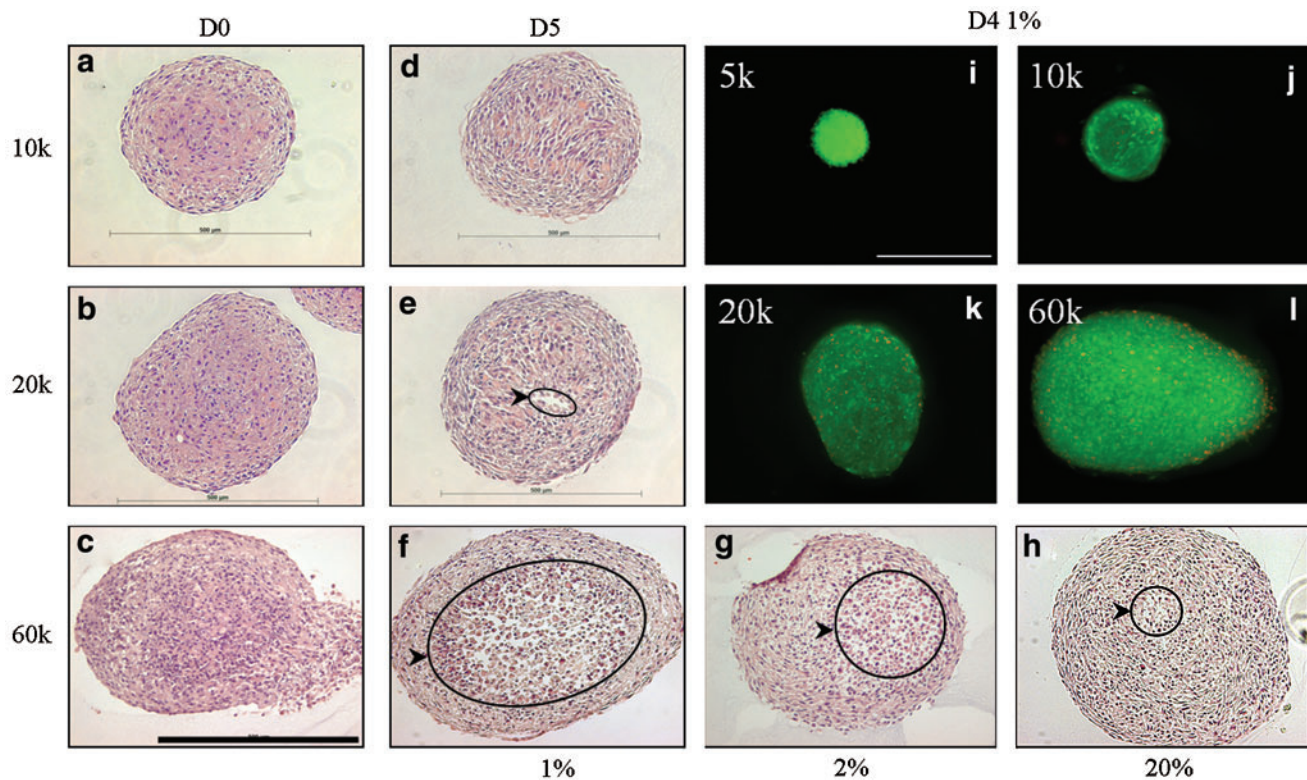


FIG. 4. (a–h) H&E staining of ADSC spheroid sections. Immediately after formation, spheroids showed high cellularity and cohesion (a–c). Cytoplasmic swelling and loss of cellular cohesion (circled regions) of central cells increased significantly with decreasing culture oxygenation in 60k spheroids (f–h). 10k and 20k spheroids incubated in 1% O<sub>2</sub> for 5 days showed little morphological change, though cellular discontinuity was seen in a small central region of some 20k spheroids (d, e). (i–l) Live/Dead viability assessment of ADSCs in 5k (i), 10k (j), 20k (k), and 60k (l) spheroids cultured at 1% O<sub>2</sub> for 4 days. Green fluorescence indicates a viable cell while red, nuclear fluorescence indicates a nonviable cell. Scale bar = 500 μm. Color images available online at [www.liebertpub.com/tea](http://www.liebertpub.com/tea)

and some cellular discontinuity was observed (g). In 1% O<sub>2</sub>, the 60k spheroids exhibited noticeable central tissue loss and a discontinuous core. Cells that did inhabit the central region all expressed cytoplasmic swelling (f). The 10k and 20k spheroids cultured in 2% and 1% O<sub>2</sub> for 5 days exhibited only minor morphological changes in some central cells but little or no loss of tissue. These spheroids cultured in 1% O<sub>2</sub> are shown in Figures 4d and e.

A LIVE/DEAD viability stain showed that on Day 1, no dead cells were observed in 5k, 10k, and 20k spheroids and only a small number were observed in 60k spheroids. As seen in Figure 4i–l, on Day 4 no dead cells were observed in 5k spheroids and only a small number of dead cells were observed in 10k spheroids. 20k and 60k spheroids displayed relatively more nonviable cells, though these still appeared to represent a small percentage of overall cells. All dead cells were located in peripheral regions of the spheroids.

## Discussion

In this work, we examined the degree of HIF activity in ADSCs cultured as spheroids of different sizes in atmospheric and reduced-oxygen conditions. We found that HIF activity increased in spheroids in a size-dependent manner and with decreasing culture oxygenation. As a well-defined HIF target, we expected VEGF to be secreted at levels that increased correspondingly with HIF activity. VEGF release profiles could be altered by changing the spheroid size, with 10k spheroids cultured in 2% or 1% O<sub>2</sub> secreting most efficiently. That spheroids larger than 10k secreted VEGF less efficiently despite having greater HIF activity may be due in part to loss of cell viability as hypoxic severity increases, as is supported by the histology. Our results indicate that culture geometry can be used as a means to control cell function and stress the need to carefully consider tissue size and expected oxygen concentration at the implant site when engineering a therapeutic graft to maximize the benefits of HIF-activated pathways.

The majority of studies in 3D stem cell cultures are carried out in atmospheric oxygenation or under a single “hypoxic” oxygen level (often 1% or 5% O<sub>2</sub>) and examine only a single culture size. We suspected that differences in culture size and external oxygen concentration (even within the hypoxic range) would significantly impact culture oxygenation and in turn affect cellular function. To test this, we prepared ADSC spheroids in a range of sizes and cultured them in three different oxygen concentrations. Centrifugal pelleting resulted in rapid formation of cohesive and spherical cultures, while providing a high degree of control over spheroid size. Additionally, a wide range of sizes could be produced (including spheroids both larger and smaller than those reported in this study). Culture size was highly reproducible and only dependent on the number of cells in the initial suspension.

HIF activity was monitored within the spheroids over 5 days. As the master regulator of transcriptional responses to low oxygen conditions, HIF activation may be the most meaningful indicator of cellular hypoxia.<sup>31</sup> Tracking HIF activity rather than oxygen concentration/distribution, as in other techniques,<sup>32–34</sup> provides evidence of a behavioral response. This is useful, as the oxygen concentration required to trigger a behavioral effect can vary between cells or even within the same cell under different microenvironmental

conditions.<sup>35,36</sup> With our HIF marker, image capture settings could be adjusted to match observed signal with quantified HIF-1 levels. Furthermore, it allowed for noninvasive identification and localization of hypoxia in cells within the 3D cultures and could follow HIF activity in the same sample over time without requiring its sacrifice. Hydrogel encapsulation facilitated consistency in repeated imaging of the same sample. While the hydrogel capsule can alter oxygen diffusion to some degree, the nature of qualitative trends observed between spheroids of different sizes was not affected. We saw that reduced oxygenation resulted in increased transcriptional activity of HIF-1 in spheroids and that increasing spheroid size amplified this effect. Quicker onset and increased intensity of fluorescent signaling was observed as culture size increased and external oxygen concentration decreased.

These results are in line with other studies: HIF-1 was shown to be exponentially stabilized in monolayer cultures as oxygen concentration decreased from 6% to 0.5%,<sup>37</sup> and higher protein levels of HIF-1 $\alpha$  were observed in ischemic mouse limb buds implanted with spheroid cultures rather than dispersed human umbilical vein endothelial cells.<sup>25</sup> Similarly, small ADSC clusters (100–200  $\mu$ m) were shown to contain higher protein levels of HIF-1 $\alpha$  than monolayer ADSCs in both 20% and 1% O<sub>2</sub>.<sup>11</sup> Our studies provided evidence on transcriptional activity of HIF-1 and examined a range of larger spheroid sizes (350–800  $\mu$ m) that better represent the size of cultures commonly prepared in osteochondral tissue engineering.

Because of the potential for a capsule to impact diffusion, spheroids for VEGF secretion studies were not encapsulated. Our results indicated that VEGF release is impacted by both external oxygenation and spheroid size, with VEGF profiles differing as these two parameters were altered. In 1% and 2% O<sub>2</sub>, 10k spheroids appeared to provide optimal secretion. Compared to cultures incubated in 20% O<sub>2</sub>, 60k, 20k, 10k, and 5k spheroids and monolayers incubated in hypoxic conditions O<sub>2</sub> showed an approximate 1.5, 3.5, 5.5, 2.5, and 2.5-fold increase in VEGF production per cell, respectively. However, in our HIF tracking studies, 20k and 60k spheroids displayed greater HIF activity than 10k spheroids. We suspect that this is due to the severity of hypoxia occurring within these spheroids, especially in the spheroid core. Severe hypoxia is known to result in a rapid and dramatic reduction in protein turnover, inhibiting protein translation and transduction.<sup>38–40</sup> Additionally, sudden, severe hypoxia can trigger apoptotic pathways or even result in cellular necrosis.<sup>41–43</sup> Results from our nuclear dye exclusion assay indicated few nonviable cells, even in 60k spheroids cultured at 1% O<sub>2</sub>. However, histological examination revealed significant acellularity and evidence of necrosis in these spheroids. This interior cell death indicates severe central hypoxia and offers an explanation for the lower than anticipated VEGF secretion from 60k and 20k spheroids.

Taken together, our data suggests that the profile of VEGF release from a 3D ADSC spheroid is the result of a balance between two opposing effects of hypoxia: (1) Decreased oxygen tension resulting from cellular oxygen utilization and diffusional limitations stabilizes HIF-1 and induces upregulation of VEGF. (2) Excessive hypoxic tension, such as increasingly occurs in the interior of spheroids as size is increased, can lead to global protein downregulation and cell

death. ADSCs have demonstrated pro-angiogenic potential and may represent a preferential source for cell-based delivery in tissue engineering and regenerative medicine. Furthermore, the benefits of 3D culture are recognized. Considering culture geometry and expected environmental oxygen concentration allow for optimization of angiogenic function of 3D ADSC cultures and will be essential to balancing the beneficial and detrimental effects of hypoxia to achieve their successful utilization in tissue engineering and regenerative medicine.

### Acknowledgments

The authors would like to thank Dr. Melissa Moss and the Instrument Resource Facility and the University of South Carolina School of Medicine for the generous use of equipment and assistance with histology. The authors would also like to acknowledge support for this work provided by a grant from the National Institutes of Health (RO3AR062816).

### Disclosure Statement

This work was funded by the National Institutes of Health (RO3AR062816).

### References

- Lovett, M., Lee, K., Edwards, A., and Kaplan, D.L. Vascularization strategies for tissue engineering. *Tissue Eng Part B Rev* **15**, 353, 2009.
- Novosel, E.C., Kleinhans, C., and Kluger, P.J. Vascularization is the key challenge in tissue engineering. *Adv Drug Deliv Rev* **63**, 300, 2011.
- Levenberg, S., Rouwkema, J., Macdonald, M., Garfein, E.S., Kohane, D.S., Darland, D.C., Marini, R., Van Blitterswijk, C.A., Mulligan, R.C., D'Amore, P.A., and Langer, R. Engineering vascularized skeletal muscle tissue. *Nat Biotechnol* **23**, 879, 2005.
- Kunz-Schughart, L.A., Schroeder, J.A., Wondrak, M., van Rey, F., Lehle, K., Hofstaedter, F., and Wheatley, D.N. Potential of fibroblasts to regulate the formation of three-dimensional vessel-like structures from endothelial cells *in vitro*. *Am J Physiol Cell Physiol* **290**, C1385, 2006.
- Blasi, A., Martino, C., Balducci, L., Saldarelli, M., Soleti, A., Navone, S.E., Canzi, L., Cristini, S., Invernici, G., Parati, E.A., and Alessandri, G. Dermal fibroblasts display similar phenotypic and differentiation capacity to fat-derived mesenchymal stem cells, but differ in anti-inflammatory and angiogenic potential. *Vasc Cell* **3**, 5, 2011.
- Halfon, S., Abramov, N., Grinblat, B., and Ginis, I. Markers distinguishing mesenchymal stem cells from fibroblasts are downregulated with passaging. *Stem Cells Dev* **20**, 53, 2011.
- Kim, Y.J., Kim, H.K., Cho, H.H., Bae, Y.C., Suh, K.T., and Jung, J.S. Direct comparison of human mesenchymal stem cells derived from adipose tissues and bone marrow in mediating neovascularization in response to vascular ischemia. *Cell Physiol Biochem* **20**, 867, 2007.
- Lee, E.Y., Xia, Y., Kim, W.S., Kim, M.H., Kim, T.H., Kim, K.J., Park, B.S., and Sung, J.H. Hypoxia-enhanced wound healing function of adipose-derived stem cells: increase in stem cell proliferation and up-regulation of VEGF and bFGF. *Wound Repair Regen* **17**, 540, 2009.
- Nie, C., Yang, D., Xu, J., Si, Z., Jin, X., and Zhang, J. Locally administered adipose-derived stem cells accelerate wound healing through differentiation and vasculogenesis. *Cell Transplant* **20**, 205, 2011.
- Kang, Y., Park, C., Kim, D., Seong, C.M., Kwon, K., and Choi, C. Unsorted human adipose tissue-derived stem cells promote angiogenesis and myogenesis in murine ischemic hindlimb model. *Microvasc Res* **80**, 310, 2010.
- Bhang, S.H., Cho, S.W., La, W.G., Lee, T.J., Yang, H.S., Sun, A.Y., Baek, S.H., Rhie, J.W., and Kim, B.S. Angiogenesis in ischemic tissue produced by spheroid grafting of human adipose-derived stromal cells. *Biomaterials* **32**, 2734, 2011.
- Bates, R.C., Edwards, N.S., and Yates, J.D. Spheroids and cell survival. *Crit Rev Oncol Hematol* **36**, 61, 2000.
- Saleh, F.A., and Genever, P.G. Turning round: multipotent stromal cells, a three-dimensional revolution? *Cytotherapy* **13**, 903, 2011.
- Baraniak, P.R., and McDevitt, T.C. Scaffold-free culture of mesenchymal stem cell spheroids in suspension preserves multilineage potential. *Cell Tissue Res* **347**, 701, 2012.
- Bhang, S.H., Lee, S., Shin, J.Y., Lee, T.J., and Kim, B.S. Transplantation of cord blood mesenchymal stem cells as spheroids enhances vascularization. *Tissue Eng Part A* **18**, 2138, 2012.
- Shweiki, D., Itin, A., Soffer, D., and Keshet, E. Vascular endothelial growth factor induced by hypoxia may mediate hypoxia-induced angiogenesis. *Nature* **359**, 843, 1992.
- Germain, S., Monnot, C., Muller, L., and Eichmann, A. Hypoxia-driven angiogenesis: role of tip cells and extracellular matrix scaffolding. *Curr Opin Hematol* **17**, 245, 2010.
- Forsythe, J.A., Jiang, B.H., Iyer, N.V., Agani, F., Leung, S.W., Koos, R.D., and Semenza, G.L. Activation of vascular endothelial growth factor gene transcription by hypoxia-inducible factor 1. *Mol Cell Biol* **16**, 4604, 1996.
- Maxwell, P.H., and Ratcliffe, P. Oxygen sensors and angiogenesis. *Semin Cell Dev Biol* **13**, 29, 2002.
- Fong, G.H. Regulation of angiogenesis by oxygen sensing mechanisms. *J Mol Med* **87**, 549, 2009.
- Rey, S., and Semenza, G.L. Hypoxia-inducible factor-1-dependent mechanisms of vascularization and vascular remodelling. *Cardiovasc Res* **86**, 236, 2010.
- Wang, G.L., Jiang, B.H., Rue, E.A., and Semenza, G.L. Hypoxia-inducible factor 1 is a basic-helix-loop-helix-PAS heterodimer regulated by cellular O<sub>2</sub> tension. *Proc Natl Acad Sci U S A* **92**, 5510, 1995.
- Brahimi-Horn, C., Berra, E., and Pouyssegur, J. Hypoxia: the tumor's gateway to progression along the angiogenic pathway. *Trends Cell Biol* **11**, S32, 2001.
- Semenza, G.L. Hypoxia-inducible factors: mediators of cancer progression and targets for cancer therapy. *Trends Pharmacol Sci* **33**, 207, 2012.
- Bhang, S.H., Lee, S., Lee, T.J., La, W.G., Yang, H.S., Cho, S.W., and Kim, B.S. Three-dimensional cell grafting enhances the angiogenic efficacy of human umbilical vein endothelial cells. *Tissue Eng Part A* **18**, 310, 2012.
- Zelzer, E., Mamluk, R., Ferrara, N., Johnson, R.S., Schipani, E., and Olsen, B.R. VEGFA is necessary for chondrocyte survival during bone development. *Development* **131**, 2161, 2004.
- Araldi, E., and Schipani, E. Hypoxia, HIFs and bone development. *Bone* **47**, 190, 2010.
- Skiles, M.L., Fancy, R., Topiwala, P., Sahai, S., and Blanchette, J.O. Correlating hypoxia with insulin secretion using a fluorescent hypoxia detection system. *J Biomed Mater Res B Appl Biomater* **97**, 148, 2011.
- Skiles, M.L., Sahai, S., and Blanchette, J.O. Tracking hypoxic signaling within encapsulated cell aggregates. *J Vis Exp* **16**, 3521, 2011.

30. Sahai, S., McFarland, R., Skiles, M.L., Sullivan, D., Williams, A., and Blanchette, J.O. Tracking hypoxic signaling in encapsulated stem cells. *Tissue Eng Part C Methods* **18**, 557, 2012.
31. Maxwell, P.H., Pugh, C.W., and Ratcliffe, P.J. Inducible operation of the erythropoietin 3' enhancer in multiple cell lines: evidence for a widespread oxygen sensing mechanism. *Proc Natl Acad Sci U S A* **90**, 2423, 1993.
32. Revsbech, N.P., and Ward, D.M. Oxygen microelectrode that is insensitive to medium chemical composition: use in an acid microbial mat dominated by cyanidium caldarium. *Appl Environ Microbiol* **45**, 755, 1983.
33. Krihak, M.K., and Shahriari, M.R. Highly sensitive, all solid state fiber optic sensor based on the sol-gel coating technique. *Electron Lett* **32**, 240, 1996.
34. Acosta, M.A., Leki, P.Y., Kostov, Y.V., and Leach, J.B. Fluorescent microparticles for sensing cell microenvironment oxygen levels within 3D scaffolds. *Biomaterials* **30**, 3068, 2007.
35. Ci, J.T., Wang, Z., Nuyten, D.S., Rodriguez, E.H., Schaner, M.E., Salim, A., Wang, Y., Kristensen, G.B., Helland, A., Børresen-Dale, A.L., Giaccia, A., Longaker, M.T., Hastie, T., Yang, G.P., van de Vijver, M.J., and Brown, P.O. Gene expression programs in response to hypoxia: cell type specificity and prognostic significance in human cancers. *PLoS Med* **3**, e47, 2006.
36. Gibbs, B.F., Yasinska, I.M., Pchejetski, D., Wyszynski, R.W., and Sumbayev, V.V. Differential control of hypoxia-inducible factor 1 activity during pro-inflammatory reactions of human haematopoietic cells of myeloid lineage. *Int J Biochem Cell Biol* **44**, 1739, 2012.
37. Jiang, B.H., Semenza, G.L., Bauer, C., and Marti, H.H. Hypoxia-inducible factor 1 levels vary exponentially over a physiologically relevant range of O<sub>2</sub> tension. *Am J Physiol* **271**, C1172, 1996.
38. Pettersen, E.O., Juul, N.O., and Rønning, O.W. Regulation of protein metabolism of human cells during and after acute hypoxia. *Cancer Res* **46**, 4346, 1986.
39. Hochachka, P.W., Buck, L.T., Doll, C.J., and Land, S.C. Unifying theory of hypoxia tolerance: molecular/metabolic defense and rescue mechanisms for surviving oxygen lack. *Proc Natl Acad Sci U S A* **93**, 9493, 1996.
40. Koumenis, C., Naczki, C., Koritzinsky, M., Rastani, S., Diehl, A., Sonenberg, N., Koromilas, A., and Wouters, B.G. Regulation of protein synthesis by hypoxia via activation of the endoplasmic reticulum kinase PERK and phosphorylation of the translation initiation factor eIF $\alpha$ . *Mol Cell Biol* **22**, 7405, 2002.
41. Greijer, A.E., and van der Wall, E. The role of hypoxia inducible factor 1 (HIF-1) in hypoxia induced apoptosis. *J Clin Pathol* **57**, 1009, 2004.
42. Kiang, J.G., and Tsen, K.T. Biology of hypoxia. *Chin J Physiol* **49**, 223, 2006.
43. Burton, T.R., and Gibson, S.B. The role of bcl-2 family member BNIP3 in cell death and disease: NIPing at the heels of death. *Cell Death Differ* **16**, 515, 2009.

Address correspondence to:

*James O. Blanchette, PhD*

*Biomedical Engineering Program*

*College of Engineering and Computing*

*University of South Carolina*

*301 Main Street, room 2C02*

*Columbia, SC 29208*

*E-mail: blanchej@cec.sc.edu*

*Received: December 19, 2012*

*Accepted: May 1, 2013*

*Online Publication Date: June 25, 2013*